Size Estimation of Protein Clusters in the Nanometer Range by Using Spatially Modulated Illumination Microscopy

U. J. Birk[1,2], **I. Upmann**[1], **D. Toomre**[3], **C. Wagner**[1] and **C. Cremer**[*,1,4,5]

[1]Kirchhoff-Institute for Physics, University of Heidelberg, D-69120 Heidelberg, Germany
[2]Inst. of Electronic Structure & Laser, FORTH, P.O. Box 1527, 71110 Heraklion, Greece
[3]Ludwig Institute for Cancer Research, Yale University School of Medicine, New Haven, USA
[4]Institute for Pharmacy and Molecular Biotechnology, University of Heidelberg, Germany
[5]Institute for Molecular Biophysics/The Jackson Laboratory, Bar Harbor, Maine, USA

A major goal of modern cell biology is the improved understanding of the three dimensional nanostructure of cellular macromolecule complexes, a goal for which a variety of research tools have been developed. Here, we describe the potential of Spatially Modulated Illumination (SMI) microscopy, a far field light optical method, to study the axial extent of fluorescently labeled protein clusters in the membrane of PtK2 cells. This is done by comparison of experimental SMI-data with the predictions of "virtual SMI-microscopy" calculations for an assumed dye distribution. Previous SMI investigations have shown that object sizes down to a few tens of nanometers can be extracted, and the method has been applied in a biological setting to determine the axial extents of nuclear nanostructures. Using these novel far field light microscopy tools at 488 nm excitation wavelength, the extension of GPI-anchored protein clusters perpendicular to the cell membrane was estimated to be (69±18) nm.

Keywords Spatially Modulated Illumination (SMI) microscopy, SMI-nanosizing, virtual microscopy, cell membrane complexes; rafts

1. Introduction

The topological analysis of the three dimensional nanostructure of biological macromolecule complexes is of basic importance for modern cell biology. It is highly desirable to develop methods for a detailed analysis of biological nanostructures in three-dimensionally conserved cells. Here, one of the basic features to be determined is the overall size of such specific complexes. Whereas atomic force microscopy and scanning near field microscopy permit size measurements of biological nanostructures on the surface with high spatial resolution, analysis of structures inside the cell would be only possible with far field light microscopy. Until recently, the far field light optical measurements were believed to be limited by the wavelength of light to about several hundreds of nanometer. However, novel approaches of light "nanoscopy" have shown that under special conditions, this barrier can be overcome [1]. One of these novel nanoscopy techniques is Spatially Modulated Illumination (SMI) far field light microscopy [2, 3]. This far field light microscopy technique was used to obtain information about the size of specifically fluorescence labeled objects with diameters ranging from a few tens of nm to ~200 nm. In a first biological application SMI-"nanosizing" was successfully applied to estimate the size of fluorescence labeled "transcription factories" [4] or of specific gene domains [5]. Here, we report that SMI-microscopy can also be used to estimate sizes of membrane associated protein complexes in intact cells. Using this method, the axial sizes of individual clustered rafts inside the PtK2 (Potorous Tridactylis type 2) cells were determined. For this a well-known lipid raft marker, an YFP-tagged GPI-anchored protein, was antibody clustered in the plasma membrane of the PtK2 fibroblast cells, giving a punctuated appearance by epifluorescence microscopy. Using SMI-microscopy, it was possible for the first time to

* * Corresponding author: e-mail: cremer@kip.uni-heidelberg.de, Phone: +49-6221-54 9252;
FAX: +49-6221-54 9112

directly estimate in three-dimensional (3D) cells the extension of the rafts markers perpendicular to the membrane.

2. Methods

2.1. The SMI-Microscope setup

The main concept of the Spatially Modulated Illumination (SMI) fluorescence microscope is that the excitation light forms an interference fringe pattern along the optical (z) axis [2, 3]. A linearly polarized excitation laser beam is split by a 50:50 beam splitter. The two collimated and counterpropagating laser beams are focused into the back focal plane of two opposing high numerical aperture objective lenses. Between the two objective lenses, the interference field or standing "wavefield" has plane wavefronts perpendicular to the optical axis and is characterized by a $\cos^2$-shape of the intensity along the axial direction. For detection of the emitted fluorescence light, a color CCD-camera is used in a setup similar to a wide field microscope. The great advantage of this system is the defined modulated excitation. For a 3D data stack, the fluorescent objects are moved through the illumination field along the optical (z) axis, and 2D images are acquired at equidistant axial positions (step size Δz = 20 nm). Axial translation is achieved by a piezo scanning stage (closed loop) with a positioning accuracy better 1 nm. It is thus possible to obtain a 3D data stack of about 100-150 images (corresponding to an object displacement of 2-3 µm along the optical axis). As a consequence, a modulated pattern of the detected fluorescence intensity along (z) is obtained for objects with an axial extension smaller than about half the excitation wavelength. Here, an Ar^+-laser with a wavelength of λ_{ex} = 488 nm ("green light") was used for the excitation. The biological samples were brought into the object space between the two objective lenses (Fig. 1a), and the integration time was set to a value between 0.4 s and 1.2 s for each acquired 2D image, resulting in a total acquisition time of 0.4 up to 3.1 min for the whole data stack.

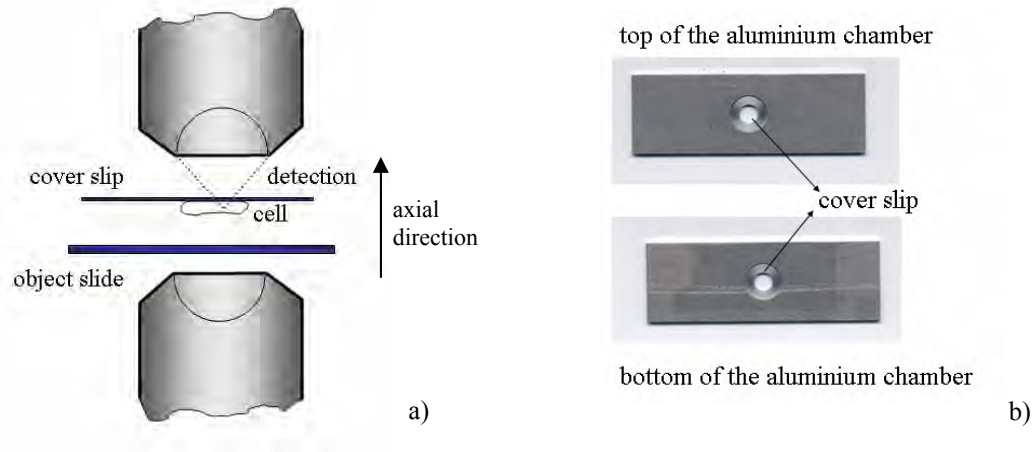

Fig. 1 Schematic representation of specimen configurations which can be inserted into the SMI-Microscope: a) Sample preparation with conventional object slide and conventional cover slip in front of the detection objective lens. b) A simple observation chamber (kindly provided by EMBL Heidelberg) using two round cover slips. This chamber allows the short term observation of live cells (used in the SMI-measurements reported here).

2.2. Preparation of the samples

"PtK2" epithelial fibroblast cells were plated on 11 mm standard cover slips (0.17 mm thick) and grown in MEM and 10% FCS at 37°C in a 5% CO_2 incubator until ~50% confluent. Cells were infected with an adenovirus that expresses an YFP labeled GPI-anchored protein, as described [6]. The so called YFP-GPI

protein has a strong affinity for rafts and is dispersed in the plasma membrane, giving a uniform appearance (not shown) when observed in a wide field fluorescence microscope. A polyclonal antibody to GFP/YFP was added to cluster these proteins in the plasma membrane for 15 min; the cells were fixed in 4% paraformaldehyde, and washed in PBS. For SMI-microscopy, the cell preparations were buffermounted between two 0.17 mm thick cover slips on custom aluminum chambers (Fig. 1b). The labeled clustered rafts in the plasma membrane had a punctuated appearance of submicron dots (c.f. Fig. 2a) and larger 'worms' (not shown). In the experiments presented here, these fluorescent microdomains within the fixed PtK2 cells were measured using the SMI-microscope to determine their axial size.

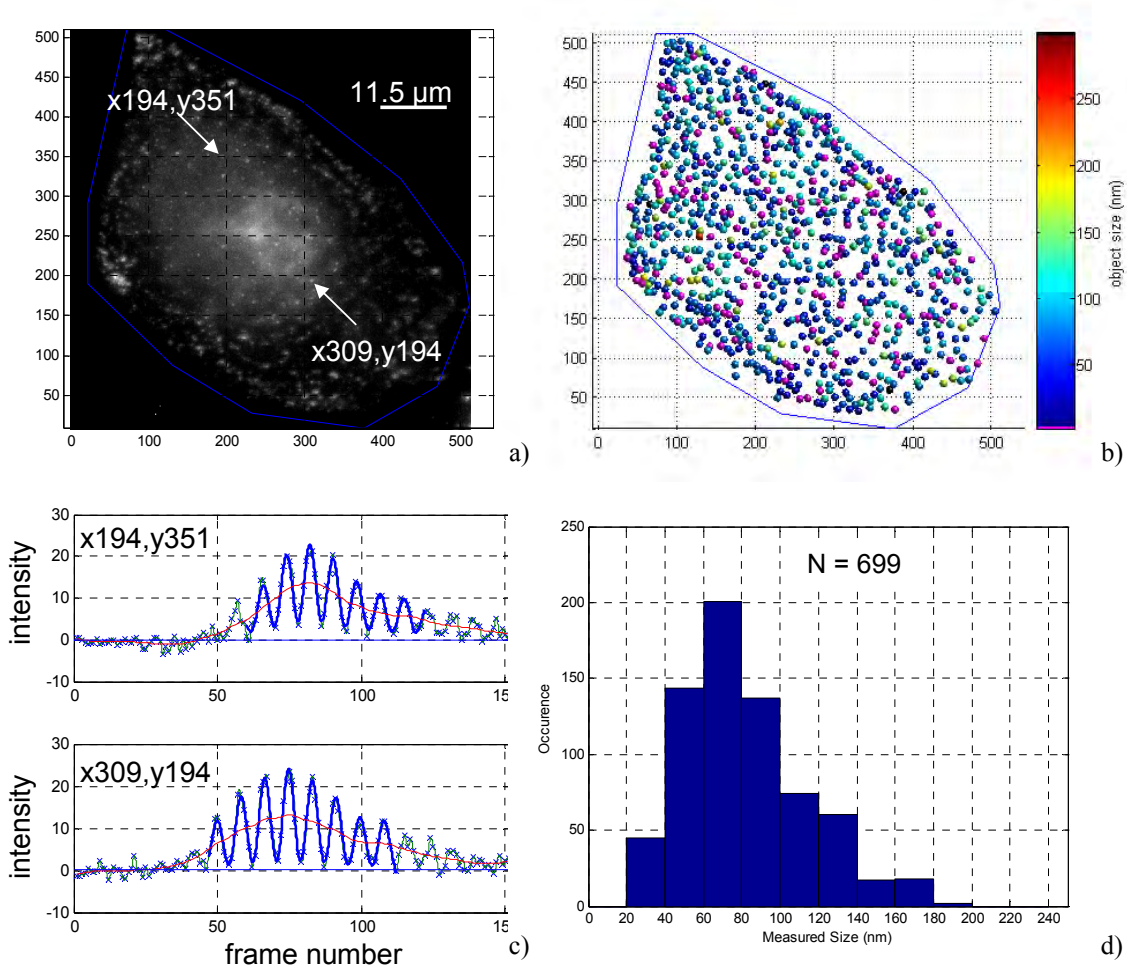

Fig. 2 Visualization of clustered GFP-tagged GPI-anchored proteins on the cell surface of a PtK2 cell. (a) Maximum intensity projection of the 3D data stack of 150 frames. (b) Color coded sizes as determined from the automatically detected points. Objects for which the evaluation failed are displayed in purple or black. The median and the standard deviation for all objects determined in this cell was (76±33) nm. (c) Intensity plots in the z-direction of the two clustered rafts at the positions (x194,y351) and (x309,y194) are shown; the upper plot corresponds to the position (x194,y351) and the lower one to the position (x309,y194). (d) Histogram of all 699 objects (single cell) for which the automated size evaluation was successful.

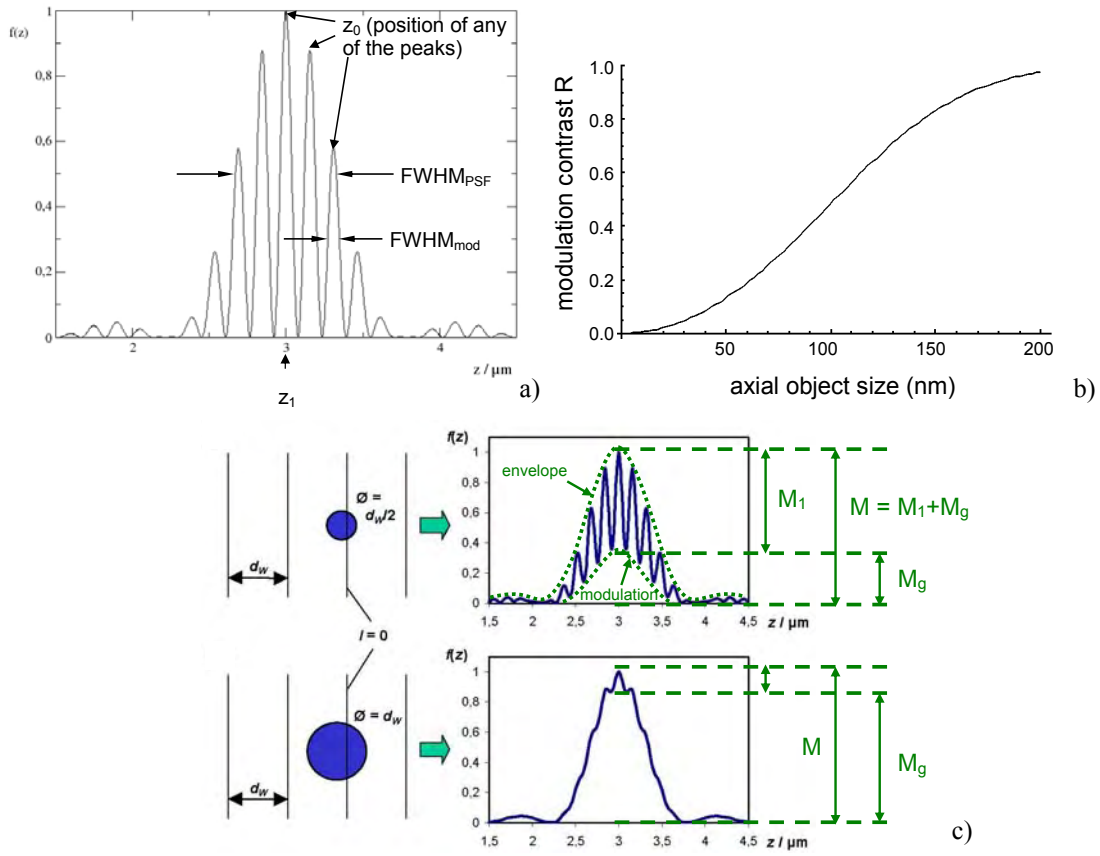

Fig. 3 The SMI-nanosizing method. a) SMI-Microscope axial Point Spread Function (cf. Eq. 1) corresponding to the Axial Intensity Distribution (AID) of a "point like" fluorescent object. b) A calibration function R(S), relating the object size S to the amount of modulation present in the AID. This curve was computed by SMI Virtual Microscopy [8] for an excitation wavelength of $\lambda = 488$ nm assuming a Gaussian dye distribution for varying object size S. c) Dependency of the AID on the object size. Top: Object size is assumed to be equal to $FWHM_{mod}$ i.e., half the distance between two wavefronts; Bottom: it is assumed to be equal to the distance of the wavefronts. As a consequence, the "disturbance" of the SMI-signal is changed [8, 9].

2.3. Concept of SMI-nanosizing

The intensity distribution of a point-like object measured with the SMI-microscope (i.e. scanning the object in axial direction through the focus) is a Point Spread Function (PSF) of which we consider in the following only the axial direction [7] i.e., the direction of the standing wave field. With the excitation wavelength of 488 nm and the refraction index of the embedding buffer medium of 1.38, the Full Width at Half Maximum ($FWHM_{mod}$) of the fringes of the standing wavefield (c.f. Fig. 3) can be calculated; $FWHM_{mod}$ is approximately 80 nm. Then all objects equal or smaller than 20 % of the calculated $FWHM_{mod}$ can be regarded as quasi "point-like" objects [8]. The total PSF of the SMI-microscope (Fig. 3a) is a product of a sinc-squared [sinc(z) = sin(z)/z] function for the wide field PSF and a cosine-squared function for the excitation PSF [8] (the standing wavefield):

$$PSF(z) = M_1 \left[\operatorname{sinc}\left(\frac{z - z_1}{B} \right) \right]^2 \cdot \left[\cos\left(\frac{z - z_0}{C} \right) \right]^2, \qquad (1)$$

where M_1, B and C are positive parameters: M_1 is the modulation amplitude; z_1 is the position of the maximum of the wide field PSF, whereas z_0 describes an arbitrary maximum of the illumination PSF. B and C are proportional to the FWHMs of the wide field PSF (B) and the modulation fringes (C) respectively.

The detected signal intensity I(z) of a non-point-like object at a given lateral (x,y) position is called the Axial Intensity Distribution (AID). The AID of an extended fluorescent object (Fig. 3c) differs from that of a "point like" object (Fig. 3a). The following adaptation function was successfully tested with commercially available fluorescent particles with various diameters provided by the manufactures [9]:

$$AID(z) = M_1 \cdot \mathrm{sinc}^2\left(\frac{z - z_1}{B}\right) \cdot \cos^2\left(\frac{z - z_0}{C}\right) + M_g \cdot \mathrm{sinc}^2\left(\frac{z - z_2}{E}\right) + L\,, \qquad (2)$$

where all parameters of the first term of the sum are the same as defined in Eq. (1). M_g and E are positive parameters; z_2 is the position of the maximum M_g of the object "disturbance". The positive parameter L corresponds to the background intensity. This adaptation function is basically a superposition of a ($\mathrm{sinc}^2 \cdot \cos^2$)-function with a second sinc^2-function. The object size (axial extension) can now be determined by calculating the modulation contrast R, which is defined as the ratio of the inner maximum of the AID and the total AID maximum ($R = M_g / (M_1 + M_g)$). For a point-like object, a complete modulation is obtained (R = 0), and the AID is equal to the PSF, whereas the modulation of the AID of an extended object is smaller (R > 0) i.e., the intensities in the local minima of the fringes are not zero. In order to obtain calibration functions, which relate the modulation contrast R to the axial extension of the fluorescent object, computer simulations ("Virtual Microscopy" – VIM [8]) were performed, using certain general assumptions about the fluorochrome distribution in the object [9]. In these simulations, the excitation and the detection PSF of the SMI-microscope are generated from the hardware parameters (e.g. excitation wavelength, numerical aperture, magnification). With the generated microscope PSFs, the intensity distributions as detected in the SMI-microscope are calculated for various differently shaped, extended objects. It is thus possible to calculate the AID of differently shaped, extended objects and to predict their modulation contrasts. In the VIM-simulations used here, it was assumed that the dye within an object is Gaussian-like distributed and the FWHM of this distribution in axial direction was considered to be the size of the object. It is also possible to compute the modulation contrast for other assumptions about the axial fluorochrome distribution [10]. Under the assumptions stated above, SMI-VIM can be utilized to determine the axial extension ("axial size") of small fluorescent objects. This is done by comparing the experimentally measured modulation contrast $R = M_g / M = M_g / (M_1 + M_g)$ with an appropriate SMI-VIM-calibration function [8-9]. This calibration function provides a functional relationship between R and the axial extension S of the objects: $R = f(S)$. We studied the dependence of the AID on the object size: With increasing object size (S) the depth of the AID modulation decreases. In the size range studied here (< 200 nm), the modulation contrast R is a monotonically increasing function of the axial object extension S. For larger objects (i.e. R close to unity), R(S) can be degenerate. However, objects with a size > 200 nm no longer show a punctiform appearance, and could thus be identified from their in-focus extension.

Figure 3b shows the modulation contrast R(S) for the popular laser excitation wavelength λ_{ex} = 488 nm. For this calibration curve a Gaussian dye distribution within the object was assumed and S represents the axial Full-Width-at-Half-Maximum (FWHM) of this distribution. For faster calculation of the modulation contrast R it is possible to neglect the detection-PSF and to consider only the total emitted light intensity of the object at different positions z in the wavefield [10]:

$$I(z) = \int_{-\infty}^{\infty} \cos^2\left(\frac{2n\pi}{\lambda}(a - z)\right) e^{-4\ln(2)a^2/d^2} da\,, \qquad (3)$$

where n is the refractive index in the object space, λ the excitation wavelength and d the FWHM (the size) of the object. By determining the minimum value (I_{min}) and the maximum value (I_{max}) of the

function I(z), the modulation contrast R can be approximated by $R = I_{min} / I_{max}$. No significant differences compared to the values obtained by the Virtual Microscopy method [8] were found when neglecting the detection PSF.

To determine the modulation contrast of the measured AIDs, a model function (Eq. 2) was fitted to the measured axial intensity distributions. To automatically find starting values for the parameters to fit, a Fourier transform of the AID was applied in a first step. The absolute value of the Fourier transformed function can be analyzed much easier than the AID itself. The obtained Fourier transformed function contains three peaks, one centered at zero frequency stemming from the envelope ($sinc^2$) and two peaks at +/- the modulation frequency (cos^2). Theory [10] showed that the intensities and the positions of these "Fourier"peaks contain all the important parameters of the AID. The parameters extracted in this way served as start values for the fit to the AID, using Eq. (2) as fit-function. This method was successfully tested using fluorescent microspheres of sizes below 100 nm.

In order to acquire a whole flat but widespread cell, the whole CCD chip (512 x 512 pixels) corresponding to an xy-area of 69 µm x 69 µm was read-out. A x-y-region of interest of 3 x 3 pixels around a randomly selected clustered raft at a site (x,y) was set to obtain the fluorescence intensity for this object in each z-slice. Plotted as a function of z, we thus obtained the modulation function (AID) of these objects as shown in Fig. 2c. From this modulation function, the modulation contrast R was extracted after fitting the model function (Eq. 2) to the AID, and from this the size was obtained as outlined above (c.f. Fig. 3b). Strictly speaking, the graphs shown in Fig. 2c are projections of a 3 x 3 ROI (corresponding to an area of 320 x 320 nm²) onto the z-axis i.e., the intensities are averaged laterally over the in-focus extent of the punctiform objects. Results obtained in this way were confirmed using test objects of known sizes ranging from 40 to 200 nm [9-10], and also by a comparative study on transcription factories using SMI and electron microscopy [4], where the average size obtained using the SMI-technique was about 15-20 nm larger than the one obtained using EM.

3. Results & Discussion

The sizes of the clustered rafts were determined from eight 3D image sequences (3D stacks, each of them containing 100 to 150 frames). The integration time per frame varied from 0.4 s to 1.2 s depending on the bleaching behavior and the intensity of the YFP signal detected. As the SMI-microscope uses a wide field detection, the Signal-to-Noise Ratio is generally much better than in conventional confocal laser scanning microscopy (CLSM). However, due to the out-of-focus illumination, bleaching could still be seen, although significantly less than in CLSM. As the in-focus modulation contrast R (i.e. the ratio between two intensities) was used to estimate the sizes, bleaching effects on the determined object sizes cancel out to a large extent. In each of the eight 3D images, ~20 regions of interest of 3 x 3 pixels were manually chosen around randomly selected fluorescence signals. Additionally, one of the acquired cell images (sequence #8) showed a good signal-to-noise ratio. This sequence could be evaluated in a fully automated way including automated detection of the fluorescence signals in the images. The mean modulation contrast R for the manual evaluation of each sequence and the corresponding standard deviation is shown in Table 1. From these modulation contrasts the sizes were calculated. The sizes determined in this way varied from 51.4 nm to 79.6 nm. The average size regarding manual evaluation of all sequences was 68.7 nm and the corresponding standard deviation amounted to 17.8 nm. During the fully automated evaluation of sequence #8, a systematically varied threshold was used to discriminate the spots. A total of 855 objects were found in a single cell (cf. Fig. 2) of which 699 were successfully analyzed (Fig. 2b). For 156 spots, equation 2 could not be fitted to the extracted AID, hence no size was obtained. The reason for this could either be the amount of noise present in the data or the limited size range (< 200 nm) for which SMI-nanosizing is feasible. For the other 699 objects in this evaluation, a median size of 76 nm and a standard deviation of 33 nm were found. Also weakly labeled objects with low intensity signal are included in this evaluation, explaining the comparably large standard deviation. Figure 2d shows a histogram of the sizes of all object evaluated for this cell.

Table 1 The mean modulation contrasts R plus the calculated sizes S for the manually selected sites are shown. The error of the modulation contrast ΔR is the standard deviation (SD) of each single measurement whereas the error of the sizes ΔS is the standard deviation (SD) of the size S[nm] for each sequence. The total number of measurements was ca. 160 whereas N is the total number of the calculated sizes of each 3D image sequence.

3D image sequence	N	R	ΔR(SD)	S [nm]	ΔS(SD) [nm]
1	19	0.385	0.100	79.6	11.3
2	20	0.326	0.136	72.7	16.1
3	18	0.313	0.188	71.1	22.5
4	20	0.302	0.148	69.8	17.9
5	18	0.339	0.195	74.2	22.9
6	20	0.167	0.089	51.4	13.4
7	19	0.199	0.142	56.2	20.1
8	19	0.342	0.167	74.6	19.6

In this report, an approach to estimate the axial size of clustered rafts in the plasma membrane of intact PtK2 fibroblast cells is presented using Spatially Modulated Illumination (SMI) microscopy. The sizes obtained are considerably higher than for the 40 nm diameter calibration objects measured previously with high reliability [9]. The present preliminary data indicate that it is possible to measure axial extensions ("sizes") of protein clusters in membranes of intact mammalian cells far beyond the conventional light microscopy optical resolution limit (several hundreds of nm), under the given circumstances (such as labeling procedures, cell preparation, relatively high background signal, out of focus contribution etc.) which affect the measurement accuracy. While other approaches with the aim to increase the axial size resolution of membrane complexes are based on focusing laser devices [11-13], here an illumination with a non-focusing "standing wave field" is applied to allow subresolution nanosizing without directly increasing the optical resolution (as defined by the FWHM of the microscope PSF). Thus, SMI-nanosizing may advantageously complement such other novel fluorescence microscopy approaches to measure the extension of membrane complexes. Our results suggest that the optical method of SMI-nanosizing, and fast extraction of the parameters with Fourier transformations, can be extended to a plethora of cellular studies where high axial size resolution is required, such as in high resolution measurements of organelles and vesicles, the cytoskeleton, parasitology and cellular morphology. For such studies, SMI-microscopy offers a robust single photon excitation optical setup (conventional object slides and cover slips can be used), a relatively fast and sensitive image acquisition (presently down to a few seconds for a complete 3D data stack) even of low fluorescence signals, combined with a large field of view (presently up to about 70 μm x 100 μm). A systematic setback in the SMI-nanosizing method, the requirement to make an assumption about the fluorochrome distribution (e.g. corresponding to a homogeneously stained flat or spherical object) can be overcome by combination with calibration measurements performed with focusing superresolving methods [11-13], with new approaches of structured illumination microscopy [14], or with localization microscopy [15].

Acknowledgements The financial supports of the Volkswagenstiftung and the Max Planck Society are gratefully acknowledged. The present studies were also supported financially from the Deutsche Forschungsgemeinschaft and the Bundesminister für Bildung und Forschung. We thank M. Bach, B. Albrecht and D. Baddeley, University Heidelberg, for stimulating discussion. U. Birk gratefully acknowledges support of his work by the European Commission (Marie Curie Fellowship).

References

[1] M. Dyba and S. W. Hell, "Focal spots of size λ/23 open up far-field florescence microscopy at 33 nm axial resolution," *Phys. Rev. Lett.* **88**, 163901 (2002).
[2] U. Spöri, A. V. Failla and C. Cremer, "Superresolution size determination in fluorescence microscopy: A comparison between spatially modulated illumination and confocal laser scanning microscopy", *Journal of Applied Physics* **95**, 8436 (2004).
[3] B. Bailey, D. L. Farkas, D. L. Taylor and F. Lanni, "Enhancement of axial resolution in fluorescence microscopy by standing-wave excitation," *Nature* **366**, 44 (1993).
[4] S. Martin, A. V. Failla, U. Spöri, C. Cremer and A. Pombo, "Measuring the size of biological nanostructures with spatially modulated illumination microscopy," *Mol. Biol. Cell* **15**, 2449 (2004).
[5] G. Hildenbrand, A. Rapp, U. Spöri, Ch. Wagner, C. Cremer and M. Hausmann, "Nano-Sizing of Specific Gene Domains in Intact Human Cell Nuclei by Spatially Modulated Illumination Light Microscopy", *Biophysical Journal Volume* **88**, 4312 (2005).
[6] K. Simons and D. Toomre, "Lipid rafts and signal transduction," *Nat. Rev. Mol. Cell Biol.* **1**, 31-39, (2000)
[7] B. Albrecht, A. V. Failla, R. Heintzmann, C. Cremer, "Spatially modulated illumination microscopy: online visualization of intensity distribution and prediction of nanometer precision of axial distance measurements by computer simulations," *J. Biomed. Opt.* **6**, 292 (2001).
[8] A. V. Failla, A. Cavallo and C. Cremer, "Subwavelength size determination by spatially modulated illumination virtual microscopy," *Appl. Opt.* **41**, 6651 (2002).
[9] A. V. Failla, U. Spoeri, B. Albrecht, A. Kroll and C. Cremer, "Nanosizing of fluorescent objects by spatially modulated illumination microscopy," *Appl. Opt*. **41**, 7275 (2002).
[10] Ch. Wagner, G. Hildenbrand, U. Spoeri and C. Cremer, Beyond Nanosizing: An Approach to Shape Analysis of Fluorescent Nanostructures by SMI-Microscopy, Optik **117,** 26 (2006).
[11] M. Dyba, J. Keller and S. W. Hell, "Phase filter enhanced STED-4Pi fluorescence microscopy: theory and experiment", *New Journal of Physics* **7**, 134 (2005).
[12] V. Westphal and S. W. Hell, "Nanoscale Resolution in the Focal Plane of an Optical Micrsocope", *Physical Review Letters* **94**, 143903 (2005).
[13] A. Egner and S. W. Hell, "Fluorescence microscopy with super-resolved optical sections, TRENDS in Cell biology **4**, 207 (2005).
[14] R. Heintzmann, Th. M. Jovin, Ch. Cremer, Saturated patterned excitation microscopy a concept for optical resolution improvement, J. Opt. Soc. Am. A, **19**, 1599 (2002).
[15] E. Betzig, G.H. Patterson, R. Sougrat, O. W. Lindwasser, S. Olenych, J. S. Bonifacino, M. W. Davidson, J. Lippincott-Schwartz, H. F. J. Hess, Imaging intracellular fluorescent proteins at nanometer resolution, Science **313**, 1642 (2006).